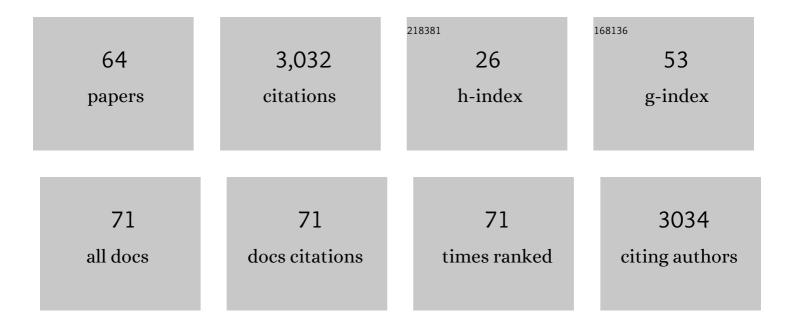
List of Publications by Year in descending order

Source: https://exaly.com/author-pdf/3588441/publications.pdf Version: 2024-02-01



#	Article	IF	CITATIONS
1	Remote sensing for agricultural applications: A meta-review. Remote Sensing of Environment, 2020, 236, 111402.	4.6	763
2	Surface energy fluxes with the Advanced Spaceborne Thermal Emission and Reflection radiometer (ASTER) at the Iowa 2002 SMACEX site (USA). Remote Sensing of Environment, 2005, 99, 55-65.	4.6	154
3	Disaggregation of MODIS surface temperature over an agricultural area using a time series of Formosat-2 images. Remote Sensing of Environment, 2010, 114, 2500-2512.	4.6	147
4	Comparison of land surface emissivity and radiometric temperature derived from MODIS and ASTER sensors. Remote Sensing of Environment, 2004, 90, 137-152.	4.6	115
5	Albedo and LAI estimates from FORMOSAT-2 data for crop monitoring. Remote Sensing of Environment, 2009, 113, 716-729.	4.6	112
6	An integrated modelling and remote sensing approach for hydrological study in arid and semiâ€∎rid regions: the SUDMED Programme. International Journal of Remote Sensing, 2008, 29, 5161-5181.	1.3	109
7	Deriving daily evapotranspiration from remotely sensed instantaneous evaporative fraction over olive orchard in semi-arid Morocco. Journal of Hydrology, 2008, 354, 53-64.	2.3	103
8	Future directions for advanced evapotranspiration modeling: Assimilation of remote sensing data into crop simulation models and SVAT models. Irrigation and Drainage Systems, 2005, 19, 377-412.	0.5	98
9	Retrieval of evapotranspiration over the Alpilles/ReSeDA experimental site using airborne POLDER sensor and a thermal camera. Remote Sensing of Environment, 2005, 96, 399-408.	4.6	93
10	A review of earth surface thermal radiation directionality observing and modeling: Historical development, current status and perspectives. Remote Sensing of Environment, 2019, 232, 111304.	4.6	91
11	Mapping surface fluxes using airborne visible, near infrared, thermal infrared remote sensing data and a spatialized surface energy balance model. Agronomy for Sustainable Development, 2002, 22, 669-680.	0.8	89
12	Detecting land cover change at the Jornada Experimental Range, New Mexico with ASTER emissivities. Remote Sensing of Environment, 2008, 112, 1730-1748.	4.6	84
13	Improvement of FAO-56 method for olive orchards through sequential assimilation of thermal infrared-based estimates of ET. Agricultural Water Management, 2008, 95, 309-321.	2.4	81
14	Estimation of land surface window (8-12 μm) emissivity from multi-spectral thermal infrared remote sensing - A case study in a part of Sahara Desert. Geophysical Research Letters, 2003, 30, .	1.5	79
15	Comparison of two temperature differencing methods to estimate daily evapotranspiration over a Mediterranean vineyard watershed from ASTER data. Remote Sensing of Environment, 2011, 115, 1326-1340.	4.6	78
16	The MISTIGRI thermal infrared project: scientific objectives and mission specifications. International Journal of Remote Sensing, 2013, 34, 3437-3466.	1.3	52
17	Remote sensing of soil surface characteristics from a multiscale classification approach. Catena, 2008, 75, 308-318.	2.2	48
18	Estimation of broadband land surface emissivity from multi-spectral thermal infrared remote sensing. Agronomy for Sustainable Development, 2002, 22, 695-696.	0.8	47

#	Article	IF	CITATIONS
19	Mapping Daily Evapotranspiration Over a Mediterranean Vineyard Watershed. IEEE Geoscience and Remote Sensing Letters, 2011, 8, 168-172.	1.4	39
20	Multidimensional Disaggregation of Land Surface Temperature Using High-Resolution Red, Near-Infrared, Shortwave-Infrared, and Microwave-L Bands. IEEE Transactions on Geoscience and Remote Sensing, 2012, 50, 1864-1880.	2.7	38
21	The utility of remotely-sensed vegetative and terrain covariates at different spatial resolutions in modelling soil and watertable depth (for digital soil mapping). Geoderma, 2013, 193-194, 83-93.	2.3	35
22	Evaporation from Heterogeneous and Sparse Canopies: On the Formulations Related to Multi-Source Representations. Boundary-Layer Meteorology, 2012, 144, 243-262.	1.2	34
23	Reassessment of the temperature-emissivity separation from multispectral thermal infrared data: Introducing the impact of vegetation canopy by simulating the cavity effect with the SAIL-Thermique model. Remote Sensing of Environment, 2017, 198, 160-172.	4.6	34
24	Management of groundwater resources in relation to oasis sustainability: The case of the Nefzawa region in Tunisia. Journal of Environmental Management, 2013, 121, 142-151.	3.8	32
25	Using remotely sensed data to estimate area-averaged daily surface fluxes over a semi-arid mixed agricultural land. Agricultural and Forest Meteorology, 2008, 148, 330-342.	1.9	30
26	Derivation of diurnal courses of albedo and reflected solar irradiance from airborne POLDER data acquired near solar noon. Journal of Geophysical Research, 2005, 110, .	3.3	27
27	Mapping short-wave albedo of agricultural surfaces using airborne PolDER data. Remote Sensing of Environment, 2002, 80, 36-46.	4.6	25
28	Spatialization of sensible heat flux over a heterogeneous landscape. Agronomy for Sustainable Development, 2002, 22, 627-633.	0.8	24
29	Multitemporal analysis of hydrological soil surface characteristics using aerial photos: A case study on a Mediterranean vineyard. International Journal of Applied Earth Observation and Geoinformation, 2012, 18, 356-367.	1.4	23
30	Impact of farmland fragmentation on rainfed crop allocation in Mediterranean landscapes: A case study of the Lebna watershed in Cap Bon, Tunisia. Land Use Policy, 2018, 75, 772-783.	2.5	23
31	Atmospheric corrections of single broadband channel and multidirectional airborne thermal infrared data: Application to the ReSeDA experiment. International Journal of Remote Sensing, 2003, 24, 3269-3290.	1.3	21
32	A three-source SVAT modeling of evaporation: Application to the seasonal dynamics of a grassed vineyard. Agricultural and Forest Meteorology, 2014, 191, 64-80.	1.9	21
33	OMERE: A Longâ€Term Observatory of Soil and Water Resources, in Interaction with Agricultural and Land Management in Mediterranean Hilly Catchments. Vadose Zone Journal, 2018, 17, 1-18.	1.3	21
34	Assessing the consistency of eddy covariance measurements under conditions of sloping topography within a hilly agricultural catchment. Agricultural and Forest Meteorology, 2012, 164, 123-135.	1.9	19
35	Mapping Biophysical Variables From Solar and Thermal Infrared Remote Sensing: Focus on Agricultural Landscapes With Spatial Heterogeneity. IEEE Geoscience and Remote Sensing Letters, 2014, 11, 1844-1848.	1.4	19
36	Observing Actual Evapotranspiration from Flux Tower Eddy Covariance Measurements within a Hilly Watershed: Case Study of the Kamech Site, Cap Bon Peninsula, Tunisia. Atmosphere, 2018, 9, 68.	1.0	18

#	Article	IF	CITATIONS
37	Modeling and Inversion in Thermal Infrared Remote Sensing over Vegetated Land Surfaces. , 2008, , 245-291.		16
38	Assessing the narrowband to broadband conversion to estimate visible, near infrared and shortwave apparent albedo from airborne PolDER data. Agronomy for Sustainable Development, 2002, 22, 537-546.	0.8	16
39	Study on thermal infrared emission directionality over crop canopies with TIR camera imagery. Science in China Series D: Earth Sciences, 2000, 43, 95-103.	0.9	15
40	Estimation of actual evapotranspiration over a rainfed vineyard using a 1-D water transfer model: A case study within a Mediterranean watershed. Agricultural Water Management, 2017, 184, 67-76.	2.4	15
41	Evaluating four gap-filling methods for eddy covariance measurements of evapotranspiration over hilly crop fields. Geoscientific Instrumentation, Methods and Data Systems, 2018, 7, 151-167.	0.6	15
42	INDO-FRENCH HIGH-RESOLUTION THERMAL INFRARED SPACE MISSION FOR EARTH NATURAL RESOURCES ASSESSMENT AND MONITORING – CONCEPT AND DEFINITION OF TRISHNA. International Archives of the Photogrammetry, Remote Sensing and Spatial Information Sciences - ISPRS Archives, 0, XLII-3/W6, 403-407.	0.2	15
43	Evaporation from multi-component canopies: Generalized formulations. Journal of Hydrology, 2013, 486, 315-320.	2.3	14
44	Accounting for vegetation height and wind direction to correct eddy covariance measurements of energy fluxes over hilly crop fields. Journal of Geophysical Research D: Atmospheres, 2015, 120, 4920-4936.	1.2	12
45	Influence of agricultural practices on micrometerological spatial variations at local and regional scales. International Journal of Remote Sensing, 2009, 30, 1183-1205.	1.3	11
46	Temperature and emissivity extracted from airborne multi-channel data in the ReSeDA experiment. Agronomy for Sustainable Development, 2002, 22, 567-573.	0.8	10
47	Estimation of surface fluxes in a small agricultural area using the three-dimensional atmospheric model Meso-NH and remote sensing data. Canadian Journal of Remote Sensing, 2003, 29, 741-754.	1.1	9
48	Use of AquaCrop model for estimating crop evapotranspiration and biomass production in hilly topography. Arabian Journal of Geosciences, 2019, 12, 1.	0.6	9
49	Comparing Landsat-7 ETM+ and ASTER Imageries to Estimate Daily Evapotranspiration Within a Mediterranean Vineyard Watershed. IEEE Geoscience and Remote Sensing Letters, 2017, 14, 459-463.	1.4	7
50	Evaluation of kernel-driven BRDF models for the normalization of Alpilles/ReSeDA POLDER data. Agronomy for Sustainable Development, 2002, 22, 531-536.	0.8	6
51	IMPACT OF LAND USE ON SOIL WATER CONTENT IN A HILLY RAINFED AGROSYSTEM: A CASE STUDY IN THE CAP BON PENINSULA IN TUNISIA. Agrofor, 2018, 3, .	0.1	5
52	First Evaluation of Land Surface Emissivity Spectra Simulated with the Sail-Thermique Model. , 2018, , .		4
53	Optimizing TRISHNA TIR channels configuration for improved land surface temperature and emissivity measurements. Remote Sensing of Environment, 2022, 272, 112939.	4.6	4
54	Estimation de l'évapotranspiration à partir de mesures de télédétection. Houille Blanche, 2002, 88, 62-67.	0.3	3

#	Article	IF	CITATIONS
55	A Simulation-Based Error Budget of the TES Method for the Design of the Spectral Configuration of the Micro-Bolometer-Based MISTIGRI Thermal Infrared Sensor. IEEE Transactions on Geoscience and Remote Sensing, 2022, 60, 1-19.	2.7	3
56	ASTER thermal infrared observations over New Mexico. , 2003, , .		2
57	Up-scaling of crop productivity estimations using the AquaCrop model and GIS-based operations. Arabian Journal of Geosciences, 2019, 12, 1.	0.6	2
58	Optimization of Instrumental Spectral Configurations for the Split-Window Method in the Context of the TRISHNA Mission. IEEE Transactions on Geoscience and Remote Sensing, 2022, 60, 1-14.	2.7	1
59	Evapotranspiration of Wheat in a Hilly Topography: Results from Measurements Using a Set of Eddy Covariance Stations. , 2017, , 67-76.		1
60	Performance of Saxton and Rawls Pedotransfer Functions for Estimating Soil Water Properties in the Cap Bon Region-Northern Tunisia. , 2017, , 77-85.		1
61	Two surface temperature retrieval methods compared over agricultural lands. , 2003, , .		0
62	Monitoring Evapotranspiration over the Alpilles Test Site by Introducing Remote Sensing Data at Various Spatial Resolutions into a Dynamic SVAT Model. AlP Conference Proceedings, 2006, , .	0.3	0
63	Relations Between Landsat Spectral Reflectances and Land Surface Emissivity Over Bare Soils. , 2019, , .		0
64	Evaluation of Ratio-Based Vegetation Indices For Annual Crops' Biomass Estimation. Lebna Watershed, Capbon, Tunisia. , 2020, , .		0